AGU PUBLICATIONS

Radio Science

RESEARCH ARTICLE
10.1002/2015RS005728

Key Points:
- A novel coordination method of opportunistic array radars
- The joint probabilistic data association algorithm of tracking is improved
- The algorithm will choose the radar which will radiate the minimum power

Correspondence to:
Z. Zhang,
zzk@nuaa.edu.cn

Citation:
Zhang, Z., S. Salous, H. Li, and Y. Tian (2015), Optimal coordination method of opportunistic array radars for multi-target-tracking-based radio frequency stealth in clutter, *Radio Sci.*, *50*, 1187–1196, doi:10.1002/2015RS005728.

Received 14 APR 2015
Accepted 29 SEP 2015
Accepted article online 24 OCT 2015
Published online 25 NOV 2015

Optimal coordination method of opportunistic array radars for multi-target-tracking-based radio frequency stealth in clutter

Zhenkai Zhang[1,2], Sana Salous[2], Hailin Li[3], and Yubo Tian[1]

[1]College of Electronic Information, JiangSu University of Science and Technology, Zhenjiang, China, [2]Centre for Communication Systems, Durham University, Durham, UK, [3]Key Laboratory of Radar Imaging and Microwave Photonics, NanJing University of Aeronautics and Astronautics, Nanjing, China

Abstract Opportunistic array radar is a new radar system that can improve the modern radar performance effectively. In order to improve its radio frequency stealth ability, a novel coordination method of opportunistic array radars in the network for target tracking in clutter is presented. First, the database of radar cross section for targets is built, then the signal-to-noise ratio for netted radars is computed according to the radar cross section and range of target. Then the joint probabilistic data association algorithm of tracking is improved with consideration of emitted power of the opportunistic array radar, which has a main impact on detection probability for tracking in clutter. Finally, with the help of grey relational grade and covariance control, the opportunistic array radar with the minimum radiated power will be selected for better radio frequency stealth performance. Simulation results show that the proposed algorithm not only has excellent tracking accuracy in clutter but also saves much more radiated power comparing with other methods.

1. Introduction

A new radar concept, the opportunistic array radar (OAR) which is also called distributed phased array radar, has been proposed by some scholars in recent years [*Jenn and Loke*, 2009; *Long et al.*, 2009; *Gong et al.*, 2013], based on digital array radar. OAR is a new radar system based on the stealth of the platform, which can improve the modern radar performance effectively. The array elements of opportunistic array radar are distributed randomly in the aircraft or ship platform. The beamforming data, control signals, and target return signals are sent wirelessly between the transmit/receive modules, where the beamformer and signal processor are located away from the modules. The concept, principle, and characteristics of the opportunistic digital array radar are presented in *Long et al.* [2009]. Phase orthogonal code sets with low autocorrelation and cross-correlation properties, which can be used in the OAR systems, are reported in *Gong et al.* [2013]. But the research of the OAR is still at the beginning, for example, there are very few studies on the radiation control of the OAR network.

Low probability intercept (LPI) is one of the important features of modern radars. In order to improve the LPI performance, we not only need to reduce the radar cross section (RCS) of the radar platform but also reduce the radiation of the radars, which is also called radio frequency stealth (RFS)[*Lynch*, 2013]. In order to achieve the important tactical requirement of RFS, dynamically controlling the emission of the radar during the radar coordination is very necessary. As we know, the less emission of the radar, the more excellent performance of the RFS. The sensor management algorithm for RFS is proposed in *Krishnamurthy* [2005], by formulation the problem as a partially observed Markov decision process with an ongoing multiarmed bandit structure. An overview of the theory, algorithms, and applications of sensor management is presented in *Hero and Cochran* [2011], as it has developed over the past decades and as it stands today. The work in *Chavali and Nehorai* [2012] computes the posterior Cramér-Rao bound on the estimates of the target state and the channel state and uses it as an optimization criterion for the antenna selection and power allocation algorithms. A joint scheme of antenna subset selection and optimal power allocation for localization is accomplished by solving a constrained optimization problem that is formulated to minimize the error in estimating target position, while conserving transmitter number and power budget [*Ma et al.*, 2014]. The paper [*Dallil et al.*, 2013] presents a new method for data association in multitarget tracking based on evidence theory. Radar detection, multitarget tracking, and data fusion techniques are applied to experimental data collected during an HF-radar experiment

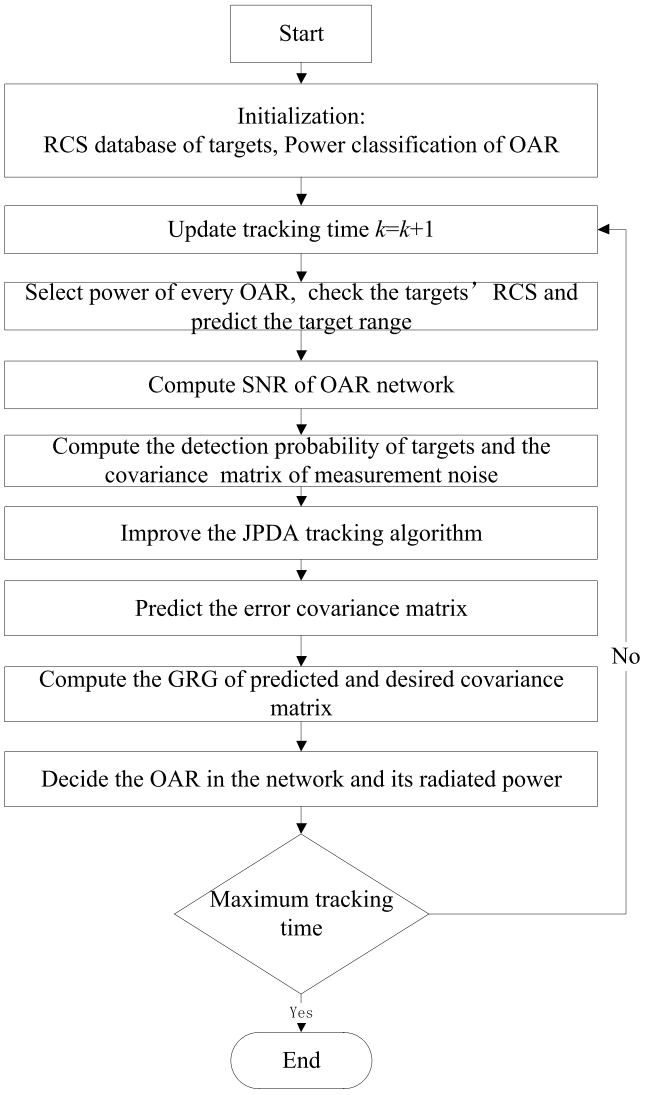

Figure 1. Procedure of the proposed algorithm.

[*Maresca et al.*, 2014], in order to solve the shortcomings such as poor range and azimuth resolution, and high nonlinearity of the sensor association. But almost all of those works concern the performance of the radars instead of RFS capability. A novel RFS optimization algorithm [*Shi et al.*, 2014a, 2014b] is presented for target tracking in radar network architectures, where Schleher intercept factor [*Lynch*, 2013] is utilized as an optimization metric for RFS performance. The paper [*Shi et al.*, 2014a, 2014b] proposes a novel RFS optimization strategy based on mutual information to improve the RFS performance for radar network. However, both of the two works control the power control problems of single target without clutter.

In this paper, a novel algorithm of power allocation for OAR networks during target tracking in clutter based on RFS is proposed. The remainder of this paper is organized as follows. Section 2 introduces the grey relation grade theory. Section 3 presents the coordination method of opportunistic array radars for multitarget track assignment in clutter. Simulations of the proposed algorithms and comparison results with other methods are provided in section 4. The conclusions are presented in section 5.

2. Grey Relational Grade Theory

In this paper, Grey relational grade (GRG) is used to measure the similarity of the desired tracking performance and actual tracking performance. Grey system theory is proposed in *Deng* [1982]. It can be used to

analyze the indeterminate and incomplete data to establish the systematic relations. GRG in grey system theory expresses the comparability between two patterns. In other words, GRG can be viewed as a measure of similarity for finite sequences and has been widely used and developed. Desired sequence Y_0 and inspected sequence Y_j are represented as $Y_0 = \{y_0(k) | k = 1,2,\ldots, n\}$ and $Y_j = \{y_j(k) | k = 1,2,\ldots, n, j = 1,2,\ldots, m\}$, respectively. The grey relational coefficient between Y_j and Y_0 at the kth component is defined as follows:

$$\varepsilon_{0j}(k) = \frac{A_1 + \zeta A_2}{\left|y_0(k) - y_j(k)\right| + \zeta A_2} \tag{1}$$

where $A_1 = \min_{j'} \min_{k'} \left|y_0(k') - y_{j'}(k')\right|$, $A_2 = \max_{j'} \max_{k'} \left|y_0(k') - y_{j'}(k')\right|$, ζ is the resolution coefficient which controls the resolution between the two distance factors, and it is also used to reduce possible influence of distortion from bias by excessive A_2. Usually, ζ is assumed as 0.5 to fit the practical requirements [*Murat and Abdulkadir,* 2015]. The average relational coefficient is the GRG, which has the form of

$$\mathrm{GRG}(Y_0, Y_j) = \frac{1}{n}\sum_{k=1}^{n} \varepsilon_{0j}(k) \tag{2}$$

In our algorithm of power control for OAR, the higher value of GRG is taken into consideration as the stronger relational degree between the predicted tracking accuracy and desired tracking accuracy. Thus, the higher GRG indicates that the predicted error covariance matrix is closer to the desired matrix, which will be described in the next section.

3. Coordination Methods of Opportunistic Array Radars for Multitarget Track Assignment in Clutter

First, the database of radar cross section (RCS) for targets is built, and the relation model between the signal-to-noise ratio (SNR) during tracking and RCS will be obtained. Then the joint probabilistic association (JPDA) algorithm of tracking is improved with the consideration of emitted power of OAR. Finally, the opportunistic array radar and its radiated power will be selected for better RFS performance, with the help of GRG and covariance control. The procedure of proposed algorithm can be shown in Figure 1.

3.1. Designing the RCS Database of the Targets for OAR

RCS is a measure of the magnitude relative to an isotropic scatterer. RCS depends on the position and orientation of the target with respect to both the source of the incident wave (e.g., the FM transmitter) and the measurement location (i.e., the radar receiver). As the array elements of OAR are distributed randomly in the platform, so the OAR can transmit and receive electromagnetic wave from different angles, and the OAR can obtain much more varieties of RCS than the conventional phased array radar, of which the array elements are distributed regularly. So the power selection method based the target RCS is more effective and suitable for OAR than conventional radars.

It is necessary to design the RCS database for OAR first. In radar applications, we are often interested in how well a target captures and reradiates electromagnetic energy. RCS is a function of size, shape, and composition of the target as well as the polarization and frequency of the incident wave. For each class within our library of potential targets, a database of RCS values (prior to tracking) corresponding to various incident and scattered directions is generated using the method in *Moulin* [2002]. The targets in this paper can be modeled as a collection of ideal scattering centers, each with value g_n and position $r_n = (x_n, y_n, z_n)$. This model is appropriate when the wavelength of the incident field is small relative to the target dimensions. In addition, each scattering center is assumed to be visible from all observation angles, the scattering from the target can be written as

$$rcs(f, \theta, \phi) = \sum_n g_n \exp[-j2\pi(Xx_n + Yy_n + Zz_n)] \tag{3}$$

where $X = \frac{2f}{c}\sin\theta\cos\varphi$, $Y = \frac{2f}{c}\sin\theta\sin\phi$, $Z = \frac{2f}{c}\cos\theta$, and (θ, ϕ) represent the incident direction in a spherical coordinate system centered on the target; f is the carrier frequency of the signal; and c is the speed of light. The capitalized notation highlights the fact that (x,y,z) and (X,Y,Z) form a Fourier transform pair. The RCS database will be built after sampling of RCS (f, θ, ϕ) is uniformed.

3.2. Computing the Signal-to-Noise Ratio and Detection Probability of OAR Network During Target Tracking

The separate RCS value for each radar pair can be obtained from the RCS database. Thermal noise at each receiver is assumed to be statistically independent. For these conditions, the overall netted radar sensitivity can be calculated by summing up the partial signal-to-noise ratio (SNR) [*Teng et al.*, 2007] of each transmitter-receiver pair (assuming that all signals can be separately distinguished at each receiver), which is given by

$$S_{NRnetted} = \sum_{i=1}^{m}\sum_{j=1}^{n} \frac{P_{t_i} G_{t_i} G_{r_j} \sigma_{ij} \lambda_i^2 t}{(4\pi)^3 k_B T_{sij} R_{ti}^2 R_{rj}^2 N_{F_j} L_{ij}} \tag{4}$$

where P_{t_i} is the ith peak transmitted power, G_{t_i} and G_{r_j} are the ith transmitter gain and jth receiver gain, σ_{ij} of the target means the ith transmitter and jth receiver which is assumed to be known in our library, λ_i is the ith transmitted wavelength, t and k_B are target integration time and Boltzmann's constant respectively, T_{sij} is the receiving system noise temperature(at a particular receiver), N_{F_j} represents the noise figure at each receiver, L_{ij} is the system loss for ith transmitter and jth receiver, R_{ti} and R_{rj} are the distance from ith transmitter to the target and distance from target to jth receiver.

Then the detection probability P_d [*Zhang and Zhou*, 2012] can be represented as

$$P_d = \exp\left(\frac{\ln P_{\text{fa}}}{1 + S_{\text{NRnetted}}}\right) \tag{5}$$

where P_{fa} is false-alarm probability. From (5), we can see that the detection probability has an important impact on the tracking performance in the clutter, which is the function of radiated power and target RCS and range.

3.3. Tracking Algorithm in the Clutter

Let $\mathbf{X}(k)$ and $\mathbf{Z}(k)$ represent the state vector and the observation vector, respectively; the state equation and transfer equation at time k are

$$\mathbf{X}(k+1) = \mathbf{F}(k+1)\mathbf{X}(k) + w(k) \tag{6}$$

$$\mathbf{Z}(k) = \mathbf{H}\mathbf{X}(k) + v(k) \tag{7}$$

where $w(k)$ and $v(k)$ are stationary white noise processes with covariance matrices $\mathbf{Q}(k)$ and $\mathbf{W}(k)$, $\mathbf{F}$ is the transition matrix and $\mathbf{H}$ is the observation matrix.

The covariance matrix $\mathbf{W}(k)$ of measurement noise is controlled by the radiated power of the OARs, RCS, and range of the target during tracking. We assume all the OARs in the network transmit the same waveform. For designing the waveform, the linear frequency modulation (LFM) combined with Gaussian pulse [*Haykin et al.*, 2011] for amplitude modulation is selected in this paper. Range and range-rate measurements are obtained using this type of waveform of which the excellent performance of range and velocity resolution is proved in *Haykin et al.* [2011] and *Cabrera* [2014]. The measurement noise covariance [*Cabrera,* 2014] is given by

$$\mathbf{W}_k = \begin{bmatrix} \dfrac{c^2 {p_u}^2}{2{S_{\text{NR}}}^k{}_{\text{netted}}} & -\dfrac{c^2 b {p_u}^2}{w_0 {S_{\text{NR}}}^k{}_{\text{netted}}} \\ -\dfrac{c^2 b {p_u}^2}{w_0 {S_{\text{NR}}}^k{}_{\text{netted}}} & \dfrac{c^2 b {p_u}^2}{w_0 {S_{\text{NR}}}^k{}_{\text{netted}}}\left(\dfrac{1}{2{p_u}^2} + 2b^2 {p_u}^2\right) \end{bmatrix} \tag{8}$$

Here c denotes the wave speed (m/s) and w_0 denotes the carrier frequency (Hz), p_u denotes the pulse length (μs) and b denotes the sweep rate (Hz/s). Paramter b can be positive (LFM upsweep), negative (LFM down-sweep), or zero. In this paper, all the waveform parameters are assumed to be constant except the signal-to-noise ratio S^k_{NRnetted} at time k.

From (4) and (8), we can see that different signal-to-noise ratio S_{NRnetted} in the radar network can lead to different measurement noise covariance. However, during the tracking process, R_{ti} and R_{rj} are unknown before radar detection in (4). So R_{ti} and R_{rj} at time k are predicted according to target's velocity, the distance from ith transmitter to the target, and distance from target to jth receiver at the last sampling time k-1. So R_{ti} and R_{rj} are replaced by R_{ti}^{pre} and R_{rj}^{pre} which are respectively presented as

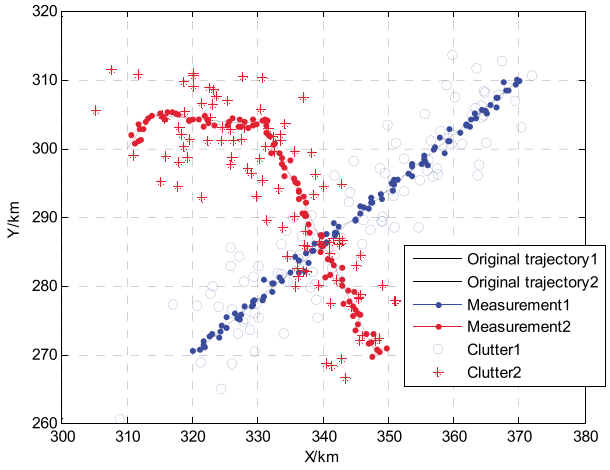

Figure 2. Trajectory and clutter environment of the two targets.

$$R_{ti}^{\mathrm{pre}}(k) = R_{ti}(k-1) + Tv_{ei}(k-1) \tag{9}$$

$$R_{rj}^{\mathrm{pre}}(k) = R_{rj}(k-1) + Tv_{ej}(k-1) \tag{10}$$

Where T is the tracking interval, $v_{ei}(k-1)$ and $v_{ej}(k-1)$ are estimated by the ith and jth OAR using the tracking algorithm at time $k-1$.

As we know, JPDA is a method of associating plots detected in the current scan with tracks using a probabilistic score, and many researchers devote their attentions [*Habtemariam et al.*, 2013; *Tae et al.*, 2015] to improve tracking accuracy in clutter under the assumption that the detection probability P_d is equal to 1. In this paper, JPDA will be improved to track the targets in clutter, with the consideration of OAR power in the network.

The update equation of the Kalman filter is

$$\mathbf{X}(k) = \mathbf{X}(k/k-1) + \mathbf{K}(k)\upsilon(k) \tag{11}$$

where $\mathbf{K}$ is the filter gain matrix and υ is the combined innovation [*Josip et al.*, 2014].

$$\upsilon(k) = \sum_{p=1}^{N_p} \beta_{tp}(k)\upsilon_{tp}(k) \tag{12}$$

where β_{tp} is the probability that plot p is originated from the target under track t, υ_{tp} is the innovation of the pth plot, and N_p is the number of plots. The updated covariance matrix is given by

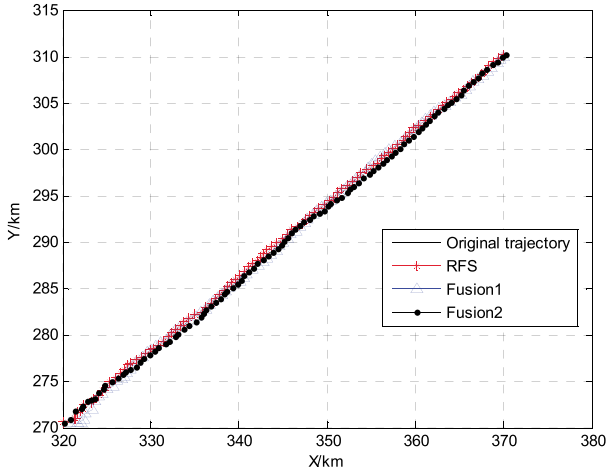

Figure 3. Tracking result of target 1.

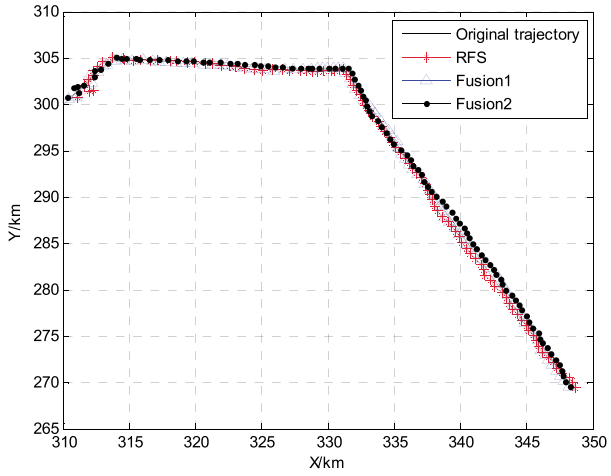

Figure 4. Tracking result of target 2.

$$\mathbf{P}(k) = \beta_0(k)\mathbf{P}(k/k-1) + [1-\beta_0(k)]\mathbf{P}^c(k/k) + \widetilde{\mathbf{P}}(k) \tag{13}$$

where

$$\widetilde{\mathbf{P}}(k) = \mathbf{K}(k)\left[\sum_{p=1}^{N_p}\beta_{tp}(k)v_{tp}(k)v_{tp}^T(k) - v(k)v^T(k)\right]\mathbf{K}^T(k) \tag{14}$$

And $\mathbf{P}^c(k/k) = [\mathbf{I} - \mathbf{K}(k)\mathbf{H}]\mathbf{P}(k/k-1)$, $\mathbf{P}$ is the error covariance matrix of the state $\mathbf{X}$, $\mathbf{I}$ is the identity matrix, and β_0 is the probability that none of the measurements in the gate originated from the target in track. The marginal association probability β_{tp} is

$$\beta_{tp} = \sum_i \mathbf{P}\{\vartheta_i | Z^k\}\hat{w}_{tp}(\vartheta_i) \tag{15}$$

where ϑ_i is a joint event (global hypothesis) and $\hat{w}_{tp}(\vartheta_i)$ is a binary variable indicating whether joint event ϑ_i contains the association of track t and plot p. The ith joint event is a hypothesis associating plots and targets at the kth scan. The probabilities of the individual joint events (joint probabilities) are given by

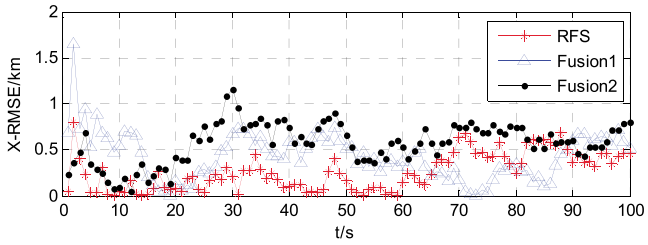

(a) Range RMSE of X direction

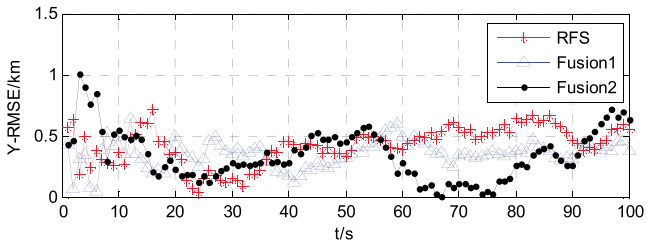

(b) Range RMSE of Y direction

Figure 5. Comparison of tracking performance of target 1.

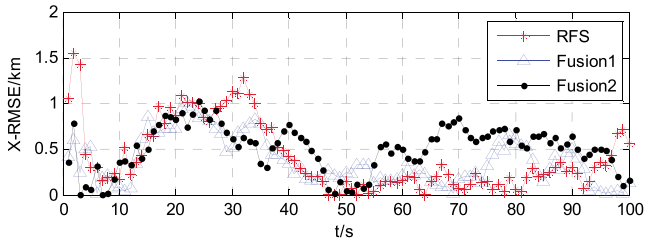

(a) Range RMSE of X direction

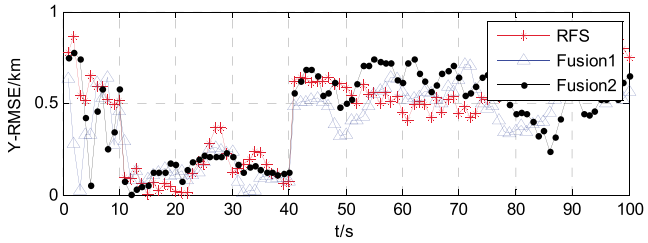

(b) Range RMSE of Y direction

Figure 6. Comparison of tracking performance of target 2.

$$\mathbf{P}\{\vartheta_i(k)|\mathbf{Z}^k\} = \frac{\rho^{\phi}}{c'}\prod_{p=1}^{N_p} \mathrm{N}_f\left[\upsilon_p(k)\right]^{\tau_p}\prod_{t=1}^{N_T}(P_D)^{\delta_t}(1-P_D)^{1-\delta_t} \tag{16}$$

where P_D is the probability of detecting the target, ϕ is the number of clutter plots, ρ is the spatial density of false measurements, δ_t is a binary variable indicating whether a track has been assigned to a plot, $\boldsymbol{N_f}$ represents the function of Normal distribution, N_T is number of current tracks, N_P is the number of plots on this scan, τ_p is a binary variable indicating whether the plot is assigned to a track and c' is a normalizing constant.

From (13) to (16), we can see the detection probability P_D has an impact on the tracking performance in clutter. So the OAR radars can radiate adaptively according to different target RCS and range in order to meet the requirement of desired tracking covariance. In (16), detection probability P_D will be obtained from the predicted signal-to-noise ratio, then the error covariance matrix $\mathbf{P}^{pre}(k)$ can be predicted through (13).

3.4. Scheduling of OARs and Their Power

Phased array elements of the opportunistic array radar are placed at available open areas over the entire length of the platform, and the elements are self-standing transmit-receive modules. As a result, it is difficult to continuously change the emitted power for every direction in real-time. We assume that a power database in every direction is already obtained. The power set which the radar m can radiate is denoted as $\mathbf{Pow^m}$,

$$\mathbf{Pow^m} = \{P^m{}_{\mathrm{av1}}, P^m{}_{\mathrm{av2}} \ldots, P^m{}_{\mathrm{avn}}\} \tag{17}$$

where $P^m_{av1} < P^m_{av2} \ldots, < P^m_{avn}$. Different radiated power from the set $\mathbf{Pow^m}$ can lead to different covariance matrix of measurement noise, which will have an impact on the result of predicted error covariance matrix.

Table 1. Comparison of Range ARMSE

	Target1		Target2	
Method	*X*-ARMSE (*km*)	*Y*-ARMSE (*km*)	*X*-ARMSE (*km*)	*Y*-ARMSE (*km*)
RFS	0.5736	0.3311	0.4188	0.4767
Fusion1	0.4315	0.3559	0.3731	0.3878
Fusion2	0.5750	0.3450	0.5129	0.4308

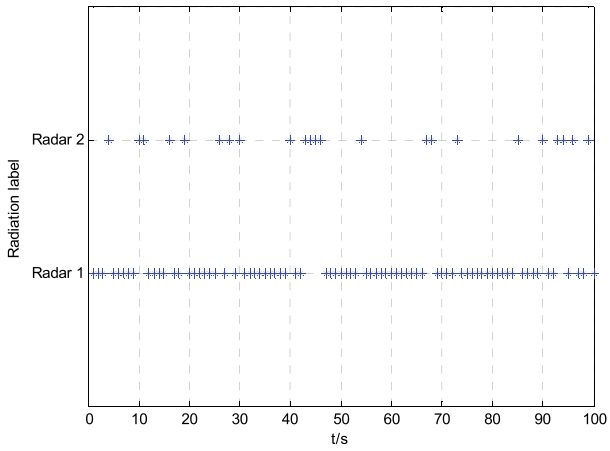

Figure 7. Radiation label of the radars.

In order to select the optimal radiated power, the desired error covariance matrix $\mathbf{P}^{\mathrm{des}}$ should be set for the M radars in the network first. The predicted error covariance matrix for mth OAR from different power in the set of $\boldsymbol{Pow}^{\mathrm{m}}$ can be obtained from (13) to (16)

$$\mathbf{P}^{\mathrm{pre}}set = \left\{\mathbf{P}_1^{\mathrm{pre}}, \mathbf{P}_2^{\mathrm{pre}} \ldots, \mathbf{P}_n^{\mathrm{pre}}\right\} \tag{18}$$

Using the Grey relational grade theory, we can obtain the GRG results between the predicted error covariance matrix and the desired matrix $\mathrm{P}^{\mathrm{des}}$:

$$\mathbf{GRG^m}\ \mathrm{set} = \left\{GRG^m{}_1, GRG^m{}_2 \ldots, GRG^m{}_n\right\} \tag{19}$$

The power $P^m{}_{\mathrm{avi}}$, which leads to the maximum grey relational grade, will be selected for the mth OAR in the network. Then a power set can be given

$$\mathbf{Pow} = \left\{P^1{}_{\mathrm{avi}}, P^2{}_{\mathrm{avj}} \ldots, P^m{}_{\mathrm{avk}}\right\} \tag{20}$$

In order to obtain best RFS performance, the algorithm will choose the radar which will radiate the minimum power in the network for tracking at time k.

4. Simulation Results

In this section, Monte Carlo simulations are performed to analyze the performance of the proposed power control method of opportunistic array radar. We use LFM with pulse length of 20 μs and sweep rate of 10^{10} Hz/s. The radar operated at a fixed carrier frequency of 10 GHz with speed of electromagnetic wave of 3×10^8m/s is employed in this paper.

4.1. Trajectory Design

We assume that there are two OARs working for the two targets tracking in clutter. The motion model of the two targets includes constant velocity model and coordinated turn rate model, and transmission matrix [*Aly et al.*, 2009] can be represented as (21) and (22), respectively.

$$F_{\mathrm{CV}} = \begin{bmatrix} 1 & T & 0 & 0 \\ 0 & 1 & 0 & 0 \\ 0 & 0 & 1 & T \\ 0 & 0 & 0 & 1 \end{bmatrix} \tag{21}$$

$$F_{\mathrm{CT}} = \begin{bmatrix} 1 & \dfrac{\sin\omega T}{\omega} & 0 & \dfrac{1-\cos\omega T}{\omega} \\ 0 & \cos\omega T & 0 & \dfrac{\sin\omega T}{\omega} \\ 0 & \dfrac{1-\cos\omega T}{\omega} & 1 & \dfrac{\sin\omega T}{\omega} \\ 0 & \sin(\omega T) & 0 & \cos\omega T \end{bmatrix} \tag{22}$$

where T is the sampling interval, ω is the turn factor, $T=1$s, and $\omega=0.1$.

Figure 2 shows the two targets trajectory with their measurement, results which are produced by the simulation in 100 s. The clutter for the every target is produced randomly during the trajectory. The positions of the radars are (50 km,150 km) and (150 km, 0 km), respectively.

4.2. Comparison of Tracking Performance

Based the GRG and JPDA methods, the proposed radiated energy algorithm for radio frequency stealth (RFS) is compared with the data fusion methods in *Dallil et al.* [2013] and *Huo* [2014], which are labeled as "Fusion1"

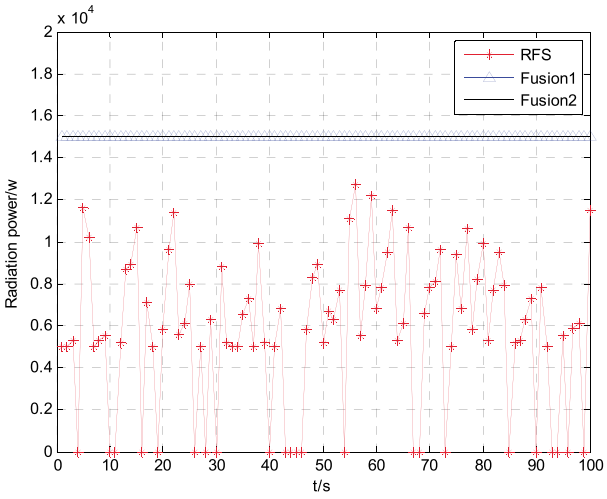

Figure 8. Comparison of radiated power of Radar 1.

and "Fusion2," respectively, in the simulation. Both algorithms are assumed to radiate the maximum power in order to get the highest detection probability, which is approximately equal to 1; the proposed method is realized with $P_d > 0.9$. The root-mean-square error (RMSE) of time k and average root-mean-square error (ARMSE) of the whole tracking process can be formulated as (23) and (24) respectively:

$$\mathrm{RMSE}(k) = \sqrt{\frac{1}{M_c}\sum_{m=1}^{M_c}\left(x_k - \hat{x}_k^m\right)^2} \tag{23}$$

$$\mathrm{ARMSE} = \frac{1}{\mathrm{N_t}}\sum_{\mathrm{k}=1}^{N_t}\mathrm{RMSE(k)} \tag{24}$$

where M_c is the number of the Monte Carlo simulation, x_k is the true state of the system, $\hat{x}_k^m$ is the estimated vector at the mth simulation, and N_t is the total tracking time in every simulation. In the simulation, $M_c = 200$, $N_t = 100$.

Figures 3 and 4 show the tracking results of two targets using the three methods. The RMSE of the two targets in X and Y direction are shown in Figures 5 and 6, respectively. Table 1 shows the ARMSE of the range. Compared with the two data fusion methods, we can see that the proposed method RFS presents almost the same excellent tracking accuracy.

4.3. Comparison of RFS Performance

As the paper focuses on the research of radar RFS ability instead of radar system design, the scattering value g_n is produced randomly with uniform distribution every time, then the RCS value can be predicted according to the tracking results and (3). The power levels in the simulation are assumed to be from 5*kw* to 15*kw* with interval of 100*w*.

The radiation label of the two opportunistic radars is shown in Figure 7. We can see that the radars work in turn. The radiated power of the radar 1 and radar 2 are illustrated in Figures 8 and 9, respectively. Compared with the two fusion methods, we can see that the proposed method not only present excellent tracking accuracy but also reduce much more radiated power.

As a result, the proposed method has better RFS ability than others. With the advantage of the transmitting and receiving property of the OAR, the radars can be selected to work according to targets' positions and RCSs in order to meet the requirement of desired tracking performance. However, the other data fusion methods are proposed to improve the tracking performance instead of the RFS ability.

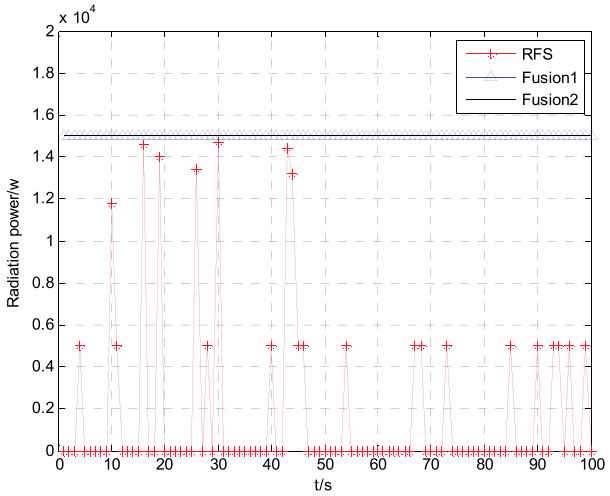

Figure 9. Comparison of radiated power of Radar 2.

5. Conclusions

In this paper, we have presented a new strategy of power control for the OAR network based on RFS. During the target tracking in the clutter, the relation model is built between the radiated power and tracking performance, as the power has an impact on the measurement noise covariance. Then the opportunistic array radar and its radiated power can be selected according to the targets' RCSs from different ranges and angles, in order

to meet the requirement of tracking performance which is measured by GRG theory. The simulation results show the proposed algorithm reduces much more radiated power with excellent tracking performance in clutter.

Acknowledgments
The authors would like to thank the anonymous reviewers for their insightful comments and suggestions that have contributed to improve this paper. We note that there are no data sharing issues since all of the numerical information is produced by solving the equations of the proposed algorithm, which are realized by MATLAB software in the paper. This work was supported by The National Natural Science Funds Fund (61401179) in China, Colleges of Jiangsu Province Natural Science Fund (14KJB510009), the Science and Technology on Electronic Information Control Laboratory Project, Scientific Research Start-up Funding from Jiangsu University of Science and Technology, and Fundamental Research Funds for the Central Universities (NJ20140010).

References

Aly, S. M., R. E. Fouly, and H. Braka (2009), Extended Kalman filtering and interacting multiple model for tracking maneuvering targets in sensor networks, *2009 Seventh Workshop on Intelligent solutions in Embedded Systems*, Ancona, 25–26 June, pp. 149–156.

Cabrera, J. B. D. (2014), Tracker-based adaptive schemes for optimal waveform selection, *2014 IEEE Radar Conference*, Cincinnati, OH, pp. 298–302, 19–23 May.

Chavali, P., and A. Nehorai (2012), Scheduling and power allocation in a cognitive radar network for multiple-target tracking, *IEEE Trans. Signal Process.*, *60*(2), 715–729.

Dallil, A., M. Oussalah, and A. Ouldali (2013), Sensor fusion and target tracking using evidential data association, *IEEE Sensor. J.*, *13*(1), 285–293.

Deng, J. L. (1982), Control problems of grey system, *Syst. Control Lett.*, *1*(5), 288–294.

Gong, S. F., W. J. Long, and H. Huang (2013), Poly phase orthogonal sequences design for opportunistic array radar via HGA, *J. Syst. Eng. Electron.*, *24*(1), 60–67.

Habtemariam, B., R. Tharmarasa, and T. Thayaparan (2013), A multiple-detection joint probabilistic data association filter, *IEEE J. Select. Top. Signal Process.*, *7*(3), 461–471.

Haykin, S., A. Zia, and Y. Xue (2011), Control theoretic approach to tracking radar: First step toward cognition, *Digit. signal Process.*, *21*, 576–585.

Hero, A. O., and D. Cochran (2011), Sensor Management: Past, Present, and Future, *IEEE Sensor. J.*, *11*(12), 3064–3075.

Huo, Y. Y. (2014), The optimal energy allocation scheme for decision fusion in heterogeneous radar sensor networks, *2014 Sixth International Conference on Wireless Communications and Signal Processing* (WCSP), pp. 1–5, Hefei, China, 23–25 Oct.

Jenn, D., and Y. Loke (2009), Distributed Phased Arrays and Wireless Beamforming Networks, *Int. J. Distrib. Sens. Network.*, *5*, 283–302.

Josip, C., M. Ivan, and J. K. Srecko (2014), Detection and tracking of dynamic objects using 3D laser range sensor on a mobile platform, *2014 11th International Conference on Informatics in Control, Automation and Robotics*, Vienna, Austria, pp. 110–119, 1–3 Sep.

Krishnamurthy, V. (2005), Emission management for low probability intercept sensors in network centric warfare, *IEEE Trans. Aerosp. Electron. Syst.*, *41*(1), 133–151.

Long, W. J., D. Ben, and M. H. Pan (2009), Opportunistic Digital Array Radar and its technical characteristic analysis, *2009 IET International Radar Conference*, Guilin, China, pp. 1–4.

Lynch, D. A. (2013), *Introduction to RF Stealth*, SciTech Publ., Raleigh, North Carolina.

Ma, B. T., H. W. Chen, and B. Sun (2014), A joint scheme of antenna selection and power allocation for localization in MIMO radar sensor networks, *IEEE Commun. Lett.*, *18*(12), 2225–2228.

Maresca, S., P. Braca, and J. Horstmann (2014), Maritime surveillance using multiple high-frequency surface–wave radars, *IEEE Trans. Geosci. Remote Sens.*, *52*(8), 5056–5071.

Moulin, H. S. (2002), A particle filtering approach to FM-band passive radar tracking and automatic target recognition, *2002 IEEE Aerospace Conference*, pp. 1789–1808.

Murat, S., and G. Abdulkadir (2015), Multi-response optimization of minimum quantity lubrication parameters using Taguchi-based grey relational analysis in turning of difficult-to-cut alloy Haynes 25, *J. Clean. Prod.*, *91*, 347–357.

Shi, C. G., J. J. Zhou, and F. Wang (2014a), Minimum mean square error based low probability of intercept optimization for radar network, *2014 IEEE International Conference on Signal Processing, Communications and Computing* (ICSPCC), Guilin, China, 5–8 Aug., pp. 10-13.

Shi, C. G., J. J. Zhou, and F. Wang (2014b), Low probability of intercept optimization for radar network based on mutual information, *2014 IEEE China Summit & International Conference on Signal and Information Processing* (ChinaSIP), Xi'an, China, 9–13 July, pp. 683-687.

Tae, H. K., D. Muslcki, and L. S. Lyul (2015), Smoothing joint integrated probabilistic data association, *IET Radar Sonar Nav.*, *9*(1), 62–66.

Teng, Y., H. D. Griffiths, and C. J. Baker (2007), Netted radar sensitivity and ambiguity, *IET Radar Sonar Nav.*, *11*(6), 479–486.

Zhang, Z. K., and J. J. Zhou (2012), A novel LPI method of radar's energy control, *Prog. Electromagn. Res. C*, *33*, 81–94.